Many-Body Methods Applied to Parity Nonconserving Transitions in Atoms: The Weak Charge and Anapole Moment of ^{133}Cs

Walter Johnson
University of Notre Dame, Notre Dame, IN (USA)
http://www.nd.edu/~johnson

1) Weak charge Q_W of ^{133}Cs provides a test of the Standard Model.

2) First (only) observation of an anapole moment was in ^{133}Cs.

3) Accurate atomic many-body calculations required.

Collaborators: M. S. Safronova, (Delaware) and U. I. Safronova (Nevada)

Atomic Parity Nonconservation

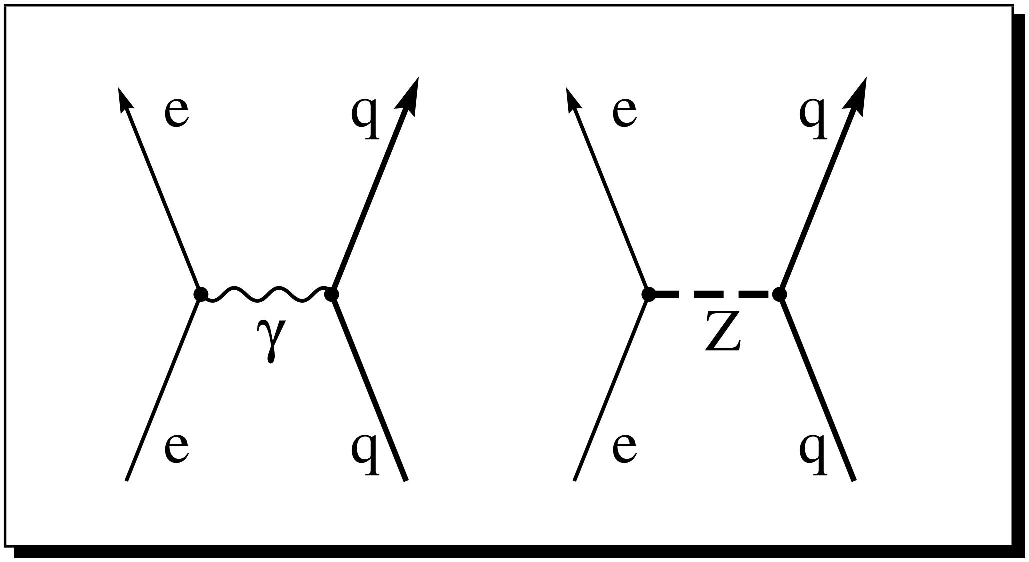

A consequence of Z exchange is that Laporte's rule "Electric dipole transitions take place only between states of opposite parity" is violated.

Laporte: http://www.nap.edu/books/0309025494/html/268.html

Otto Laporte (1902-1971) discovered the law of parity conservation in physics. He divided states of the iron spectrum into two classes, even and odd, and found that no radiative transitions occurred between like states.[1]

[1] O. Laporte, Z. Physik **23** 135 (1924).

Z Exchange in the Standard Model[2]

$$H_{\mathsf{PV}} = \frac{G}{\sqrt{2}} \Big[\bar{e}\gamma_\mu\gamma_5 e \left(c_{1u}\, \bar{u}\gamma_\mu u + c_{1d}\, \bar{d}\gamma_\mu d + \cdots \right) + \bar{e}\gamma_\mu e \left(c_{2u}\, \bar{u}\gamma_\mu\gamma_5 u + c_{2d}\, \bar{d}\gamma_\mu\gamma_5 d + \cdots \right) \Big]$$

where $\cdots = t,\ b,\ s,\ c$

$$c_{1u} = -\frac{1}{2} + \frac{4}{3}\ \sin^2\theta_W \qquad c_{1d} = \frac{1}{2} - \frac{2}{3}\ \sin^2\theta_W$$

$$c_{2u} = -\frac{1}{2}\left(1 - 4\ \sin^2\theta_W\right) \qquad c_{2d} = \frac{1}{2}\left(1 - 4\ \sin^2\theta_W\right)$$

---

[2] W. J. Marciano in *Precision Tests of the Standard Electroweak Model*, Ed. P. Langacker, (World Scientific, Singapore, 1995), p. 170.

Electron Axial-Vector – Nucleon Vector

Contribution of *coherent* vector nucleon current:

$$H^{(1)} = \frac{G}{2\sqrt{2}}\gamma_5\, Q_W\, \rho(r)$$

where $\rho(r)$ is a nuclear density ($\sim$ neutron density) and

$$\begin{aligned} Q_W &= 2[(2Z+N)c_{1u} + (Z+2N)c_{1d}] \\ &= -N + Z\,(1 - 4\,\sin^2\theta_W) \\ &\sim -N \end{aligned}$$

Electron Vector – Nucleon Axial-Vector

Contribution of vector axial-vector nucleon current:

$$H^{(2)} = -\frac{G}{\sqrt{2}} \boldsymbol{\alpha} \cdot \left[c_{2p} \left\langle \phi_p^\dagger \boldsymbol{\sigma} \phi_p \right\rangle + c_{2n} \left\langle \phi_n^\dagger \boldsymbol{\sigma} \phi_n \right\rangle \right]$$

where $\langle \cdots \rangle$ designates nuclear matrix elements.

$$c_{2p} \sim 1.25 \times c_{2u} = -0.068$$
$$c_{2n} \sim 1.25 \times c_{2d} = 0.068$$

Shell Model Estimates

$$H^{(2)} = \frac{G}{\sqrt{2}}\, \kappa_2\ \alpha \cdot \mathbf{I}\, \rho(r)$$

κ_2 from "Extreme" Shell Model and from Recent Calculations.[3]

Element	A	State	κ_2	Ref. [3]]
K	39	$1d_{3/2}\ (p)$	0.0272	
Cs	133	$1g_{7/2}\ (p)$	0.0151	0.0140
Ba	135	$2d_{3/2}\ (n)$	-0.0272	
Tl	205	$3s_{1/2}\ (p)$	-0.136	-0.127
Fr	209	$1h_{9/2}\ (p)$	0.0124	

[3] W. C. Haxton, C.-P. Liu, and M. J. Ramsey-Musolf, Phys. Rev. Lett. **86**, 5247 (2001).

Nuclear Anapole Moment

PNC in nucleus $\Rightarrow$ nuclear anapole:

$$\boldsymbol{A} = \boldsymbol{a}\, \delta(\boldsymbol{r})$$

$$\boldsymbol{a} = -\pi \int d^3r\, r^2\, \boldsymbol{j}(\boldsymbol{r}) = \frac{1}{e}\, \frac{G}{\sqrt{2}}\, \kappa_a \boldsymbol{I}$$

$$\boxed{H^{(a)} = e\, \boldsymbol{\alpha} \cdot \boldsymbol{A} \rightarrow \frac{G}{\sqrt{2}}\, \kappa_a\, \alpha \cdot \mathbf{I}\, \rho(r)}$$

Early estimates[4] for ^{133}Cs gave $\kappa_a = 0.063 - 0.084.$ Recent estimates given in[5]

[4] V. V. Flambaum, I. B. Khriplovich, O. P. Sushkov Phys. Letts. B **146** 367-369 (1984).

[5] V. V. Flambaum and D. W. Murray, Phys. Rev. C**56**, 1641 (1997); W. C. Haxton and C. E. Wieman, Ann. Rev. Nucl. Part. Sci. **51**, 261 (2001)

Spin-Dependent Interference Term

According to Flambaum and Khriplovich[6] and Bronchiat and Piketty,[7] interference between the hyperfine interaction H_{hf} and $H^{(1)}$ gives another nuclear spin-dependent correction of the form

$$H^{(\mathrm{hf})} = \frac{G}{\sqrt{2}} \kappa_{\mathrm{hf}} \, \alpha \cdot \mathbf{I} \, \rho(r)$$

$$^{133}\mathrm{Cs:} \quad \kappa_{\mathrm{hf}} = 0.0078$$
$$^{205}\mathrm{Tl:} \quad \kappa_{\mathrm{hf}} = 0.044$$

$$\kappa_{\mathrm{hf}} \sim \tfrac{1}{2}\, \kappa_2$$

[6] V. V. Flambaum and I. B. Khriplovich, Sov. Phys. JETP **62**, 872 (1985).
[7] C. Bouchiat and C. A. Piketty, Z. Phys. C 49, 91 (1991); Phys. Lett. B 269, 195 (1991).

Optical Rotation Experiments

Aim is to measure $E_{\text{PNC}} = \langle f|z|i\rangle \propto Q_W$:

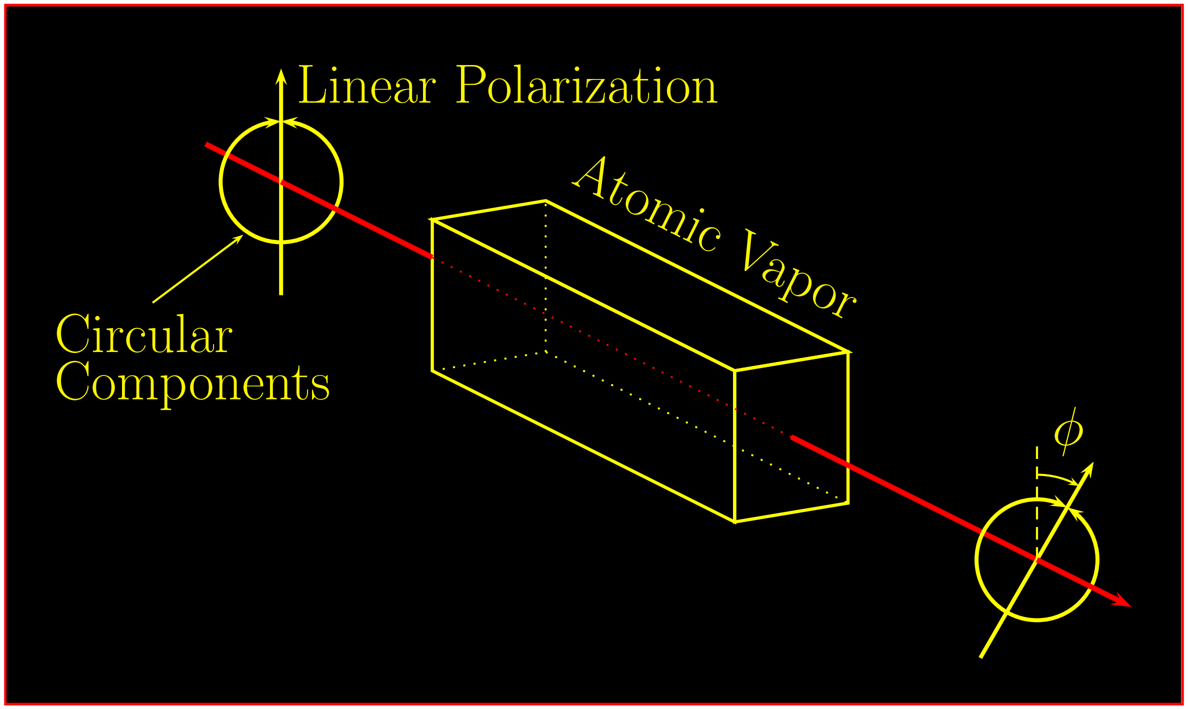

The plane of polarization of a linearly polarized laser beam passing through a medium with $n_+ \neq n_-$ is rotated. The rotation angle $\phi \propto R_\phi = \text{Im}\left(E_{\text{PNC}}\right)/M1$.

Optical Rotation Experiments-II

$$R_\phi = \mathrm{Im}\left(E_{\mathrm{PNC}}\right)/M1$$

Measured values of R_ϕ

Element	Transition	Group	$10^8 \times R_\phi$
^{205}Tl	$^2P_{1/2} - {}^2P_{3/2}$	Oxford (95)	-15.33(45)
^{205}Tl	$^2P_{1/2} - {}^2P_{3/2}$	Seattle (95)	-14.68(20)
^{208}Pb	$^3P_0 - {}^3P_1$	Oxford (94)	-9.80(33)
^{208}Pb	$^3P_0 - {}^3P_1$	Seattle (95)	-9.86(12)
^{209}Bi	$^4S_{3/2} - {}^2D_{3/2}$	Oxford (91)	-10.12(20)

Stark-Interference Experiment

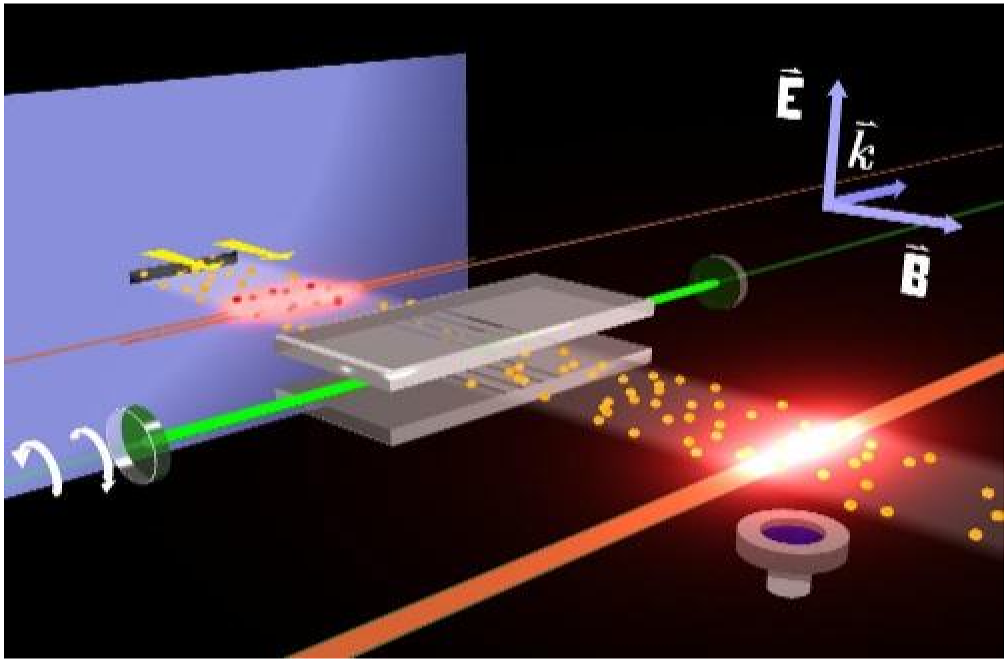

Boulder PNC apparatus: A beam of cesium atoms is optically pumped by diode laser beams, then passes through a region of perpendicular electric and magnetic fields where a green laser excites the transition from the 6S to the 7S state. The excitations are detected by observing the florescence (induced by another laser beam) with a photo-diode.

Stark-Interference Experiments II

Evolving values of $R = \text{Im}\left(E_{\text{PNC}}\right)/\beta$ (mV/cm) for ^{133}Cs			
Transition	Group	R_{4-3}	R_{3-4}
$6s_{1/2} - 7s_{1/2}$	Paris (1984)	-1.5(2)	-1.5(2)
$6s_{1/2} - 7s_{1/2}$	Boulder (1988)	-1.64(5)	-1.51(5)
$6s_{1/2} - 7s_{1/2}$	Boulder (1997)	-1.635(8)	-1.558(8)

The vector current contribution from the last row is

$$R_{\text{Stark}} = -1.593 \pm 0.006$$

$$\text{Im}\left[E_{\text{PNC}}(6s \rightarrow 7s) \times 10^{11}\right] = -0.8376 \pm (0.0031)_{\text{exp}} \pm (0.0021)_{\text{th}}$$

Other Experiments

Element	Transition	Group
Fr	$7S_{1/2} \rightarrow 8S_{1/2}$	Stony Brook
Fr	$7S_{1/2}[F=4] \rightarrow 7S_{1/2}[F=5]$	Stony Brook
Yb	$(6s^2)\,^1S_0 \rightarrow (6s5d)\,^3D_1$	Berkeley
Yb	$(6s6p)\,^3P_0 \rightarrow (6s6p)\,^3P_1$	Berkeley
Ba^+	$6S_{1/2} \rightarrow 5D_{3/2}$	Seattle
Dy	$(4f^{10}5d6s)[10] \rightarrow (4f^9 5d^2 6s)[10]$	Berkeley
Sm	$(4f^6 6s^2)\,^7F_J \rightarrow (4f^6 6s^2)\,^5D_{J'}$	Oxford

Calculations of the $6s \rightarrow 7s$ Amplitude in Cs

- Perturbation theory in the screened Coulomb interaction.[8] Important classes of diagrams are summed to all orders.
- SD method (linearized coupled cluster) discussed earlier. [9]
- Nonlinear coupled-cluster calculations by B. Das (unpublished).[10]

Theoretical values for E_{PNC} Units: $i(-Q_W/N) \times 10^{-11} ea_0$

PTSCI	-0.908 (5)
SDCC	-0.909 (4)
B. Das	-0.911

[8] V. A. Dzuba, V. V. Flambaum, and J. S. M. Ginges, Phys. Rev. D **66**, 076013 (2002).

[9] S. A. Blundell et al., Phys. Rev. D**45**, 1602 (1992).

[10] `http://mocha.phys.washington.edu/~int_talk/WorkShops/int_02_3/People/Das_B/`

SD Calculation of PNC amplitude

$$E_{\mathrm{PNC}} = \sum_n \frac{\langle 7s|D|np\rangle\langle np|H^{(1)}|6s\rangle}{E_{6s} - E_{np}} + \sum_n \frac{\langle 7s|H^{(1)}|np\rangle\langle np|D|6s\rangle}{E_{7s} - E_{np}}$$

"Weak" RPA gives E_{PNC} accurate to about 3%. Therefore, we organize calculation as follows:

- $n = 6 - 9$ valence states: evaluate matrix elements using SD wave functions (99%)
- $n = 1 - 5$ core states and $n > 10$: evaluate using "weak" RPA amplitudes (1%)

Contributions to PNC Amplitude

Contributions to E_{PNC} in units $-iea_0Q_W/N$.

n	$\langle 7s\|D\|np\rangle$	$\langle np\|H^{(1)}\|6s\rangle$	$E_{6s}-E_{np}$	Contrib.
6	1.7291	-0.0562	-0.05093	1.908
7	4.2003	0.0319	-0.09917	-1.352
8	0.3815	0.0215	-0.11714	-0.070
9	0.1532	0.0162	-0.12592	-0.020
n	$\langle 7s\|\|H^{(1)}\|np\rangle$	$\langle np\|D\|6s\rangle$	$E_{7s}-E_{np}$	Contrib.
6	-1.8411	0.0272	0.03352	-1.493
7	0.1143	-0.0154	-0.01472	0.120
8	0.0319	-0.0104	-0.03269	0.010
9	0.0171	-0.0078	-0.04147	0.003
$n=6-9$				-0.894(4)
RPA part				-0.015(1)
Total				-0.909(4)

Brueckner-Goldstone Diagrams for the SDCC Equations

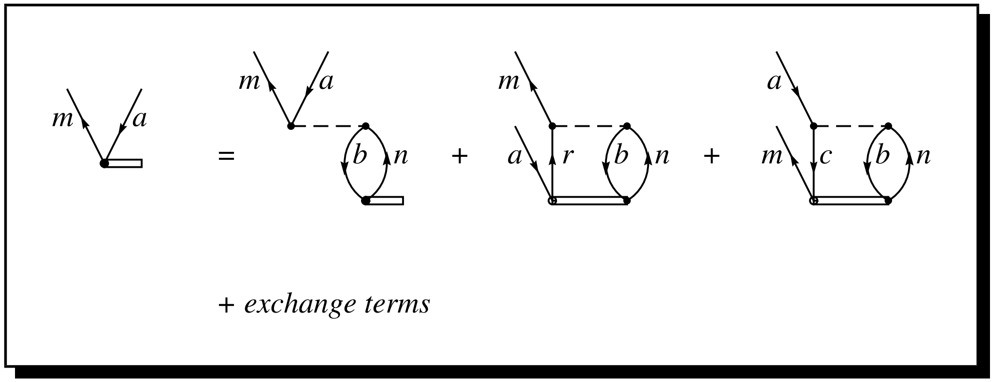

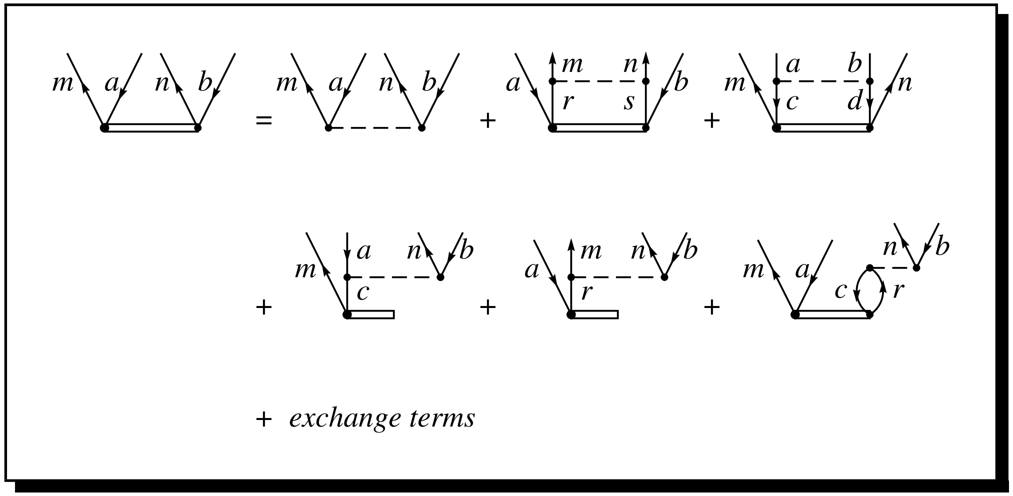

Analysis of $6s \rightarrow 7s$ Amplitude in ^{133}Cs

Combining the calculations and the measurements

$$Q_W^{\text{exp}}(^{133}\text{Cs}) = -71.91(46)$$

differs with the standard model value

$$Q_W^{\text{SM}}(^{133}\text{Cs}) = -73.09(3)$$

by 2.5 σ

Additional Corrections:

- Breit interaction -0.6%
- Vacuum Polarization +0.4%
- αZ Vertex Corrections -0.7%
- Nuclear Skin Effect -0.2%

Analysis of $6s \rightarrow 7s$ Amplitude in ^{133}Cs

Combining the calculations and the measurements

$$Q_W^{\text{exp}}(^{133}\text{Cs}) = -71.91(46) \quad \Rightarrow -72.73(46)$$

differs with the standard model value

$$Q_W^{\text{SM}}(^{133}\text{Cs}) = -73.09(3)$$

by 2.5 σ $\Rightarrow$ 0.8 σ

Additional Corrections:

- Breit interaction -0.6%
- Vacuum Polarization +0.4%
- αZ Vertex Corrections -0.7%
- Nuclear Skin Effect -0.2%

Angular Momentum Considerations

$$\langle F\|z\|I\rangle^{(1)} = (-1)^{j_F+F_I+I+1}\sqrt{[F_I][F_F]}\left\{\begin{array}{ccc} F_F & F_I & 1 \\ j_I & j_F & I \end{array}\right\}$$

$$\times \sum_{n j_n}\left[\frac{\langle j_F\|z\|n\, j_n\rangle\langle n\, j_n\|H^{(1)}\|j_I\rangle}{E_I - E_n} + \frac{\langle j_F\|H^{(1)}\|n\, j_n\rangle\langle n\, j_n\|z\|j_I\rangle}{E_F - E_n}\right]$$

$$\langle F\|z\|I\rangle^{(2)} = \sqrt{I(I+1)}\sqrt{[I][F_I][F_F]}\times$$

$$\sum_{n j_n}\left[(-1)^{j_I-j_F+1}\left\{\begin{array}{ccc} F_F & F_I & 1 \\ j_n & j_F & I \end{array}\right\}\left\{\begin{array}{ccc} I & I & 1 \\ j_n & j_I & F_I \end{array}\right\}\right.$$

$$\times \frac{\langle j_F\|z\|n\, j_n\rangle\langle n\, j_n\|H^{(2)}\|j_I\rangle}{E_I - E_n}$$

$$+ (-1)^{F_I-F_F+1}\left\{\begin{array}{ccc} F_F & F_I & 1 \\ j_I & j_n & I \end{array}\right\}\left\{\begin{array}{ccc} I & I & 1 \\ j_n & j_F & F_F \end{array}\right\}$$

$$\left.\times \frac{\langle j_F\|H^{(2)}\|n\, j_n\rangle\langle n\, j_n\|z\|j_I\rangle}{E_F - E_n}\right]$$

Matrix Element (10^{-11})	$H^{(1)}$	$H^{(2)}$	$\epsilon_{F'F}$
$\langle 7s\ [3]\ \|\|\ z\ \|\| 6s\ [3]\rangle$	-2.037	-0.2250	0.1105
$\langle 7s\ [3]\ \|\|\ z\ \|\| 6s\ [4]\rangle$	-3.528	-0.7296	0.2068
$\langle 7s\ [4]\ \|\|\ z\ \|\| 6s\ [3]\rangle$	3.328	-0.6430	-0.1823
$\langle 7s\ [4]\ \|\|\ z\ \|\| 6s\ [4]\rangle$	2.981	-0.2562	-0.0859

$$E^{\text{exp}}_{\text{PNC}} = E^{(1)}_{\text{PNC}} \left[\frac{Q_W}{-N} + \kappa\ \epsilon_{F'F} \right]$$

β (a_0^3)	27.024(80)
$E^{\text{exp}}_{34}/\beta$ (mV/cm)	-1.6349(80)
$E^{\text{exp}}_{43}/\beta$ (mV/cm)	-1.5576(77)
E^{exp}_{34} (10^{-11})	-0.8592(49)
E^{exp}_{43} (10^{-11})	-0.8186(47)
$E^{\text{exp}}_{\text{V}}$ (10^{-11})	-0.8376(37)
$E^{(1)}_{\text{PNC}}$ (10^{-11})	-0.9085(45)
Q^{exp}_W	-71.91(46)
κ^{exp}	0.117(16)

Weak-Hyperfine Interference

$$Z_{wv}^{(\mathsf{hf})} = \sum_{\substack{i\neq w \\ j\neq v}} \left[\frac{(H^{(1)})_{wi}\; z_{ij}\; (H_{\mathsf{hf}})_{jv}}{(\epsilon_i - \epsilon_w)(\epsilon_j - \epsilon_v)} + \frac{(H_{\mathsf{hf}})_{wi}\; z_{ij}\; (H^{(1)})_{jv}}{(\epsilon_i - \epsilon_w)(\epsilon_j - \epsilon_v)} \right]$$

$$+ \sum_{\substack{i\neq v \\ j\neq v}} \left[\frac{z_{wi}\; (H^{(1)})_{ij}\; (H_{\mathsf{hf}})_{jv}}{(\epsilon_i - \epsilon_v)(\epsilon_j - \epsilon_v)} + \frac{z_{wi}\; (H_{\mathsf{hf}})_{ij}\; (H^{(1)})_{jv}}{(\epsilon_i - \epsilon_v)(\epsilon_j - \epsilon_v)} \right]$$

$$+ \sum_{\substack{i\neq w \\ j\neq w}} \left[\frac{(H^{(1)})_{wj}\; (H_{\mathsf{hf}})_{ji}\; z_{iv}}{(\epsilon_i - \epsilon_w)(\epsilon_j - \epsilon_w)} + \frac{(H_{\mathsf{hf}})_{wj}\; (H^{(1)})_{ji}\; z_{iv}}{(\epsilon_i - \epsilon_w)(\epsilon_j - \epsilon_w)} \right]$$

$$- \sum_{i\neq v} \frac{z_{wi}\; (H^{(1)})_{iv}}{(\epsilon_i - \epsilon_v)^2}\; (H_{\mathsf{hf}})_{vv} \;-\; (H_{\mathsf{hf}})_{ww} \sum_{i\neq w} \frac{(H^{(1)})_{wi}\; z_{iv}}{(\epsilon_i - \epsilon_w)^2}$$

Analysis of κ_{hf} for ^{133}Cs

Dipole Matrix Element	$H^{(2)}$	$H^{(1)} \times H_{\text{hf}}$	$\sim \kappa_{\text{hf}}$
$\langle 7s\ [3]\ \|\| z \|\| 6s\ [3] \rangle$	2.249[-12]	1.141[-14]	5.076[-03]
$\langle 7s\ [3]\ \|\| z \|\| 6s\ [4] \rangle$	7.299[-12]	3.579[-14]	4.903[-03]
$\langle 7s\ [4]\ \|\| z \|\| 6s\ [3] \rangle$	6.432[-12]	3.139[-14]	4.880[-03]
$\langle 7s\ [4]\ \|\| z \|\| 6s\ [4] \rangle$	2.560[-12]	1.300[-14]	5.076[-03]

Thus, for the $7s - 6s$ transition in ^{133}Cs, we can describe the interference term approximately as $H^{(\text{hf})} = \kappa_{\text{hf}}\, \boldsymbol{\alpha} \cdot \boldsymbol{I} \rho(\boldsymbol{r})$ with $\kappa_{\text{hf}} = 0.0049$.

- ⋆ $H^{(2)}$ is sensitive to correlations, Hyperfine term is not.
- ⋆ Hyperfine term is sensitive to negative-energy states, $H^{(2)}$ is not.

Anapole Moment of ^{133}Cs

Group	κ	κ_2	κ_{hf}	κ_a
Present	0.117(16)	0.0140[1]	0.0049	0.098(16)
Haxton *et al.*	0.112(16)[2]	0.0140	0.0078[3]	0.090(16)
Flambaum and Murray	0.112(16)[4]	0.0111[5]	0.0071[6]	0.092(16)[7]
Bouchiat and Piketty		0.0084	0.0078	

[1] from Haxton *et al.*

[2] from Flambaum and Murray

[3] from Bouchiat and Piketty

[4] The spin-dependent matrix elements from Kraftmakher are used.

[5] Shell-model value with $\sin^2\theta_W = 0.23$.

[6] This value was obtained by scaling the analytical result from Flambaum and Khriplovich ($\kappa_{\text{hf}} = 0.0049$) by a factor 1.5.

[7] Contains a 1.6% correction for finite nuclear size; the raw value is 0.094(16).

Evaluation of the Anapole Moment

The (low-energy) parity nonconserving nucleon-nucleon interaction is conventionally described by a one-meson exchange potential having one strong-interaction vertex $\{g_{\pi NN}, g_\rho, g_\omega\}$ and one weak vertex $\{f_\pi,\ h^0_\rho,\ h^1_\rho,\ h^2_\rho,\ h^0_\omega,\ h^1_\omega\}$[11]

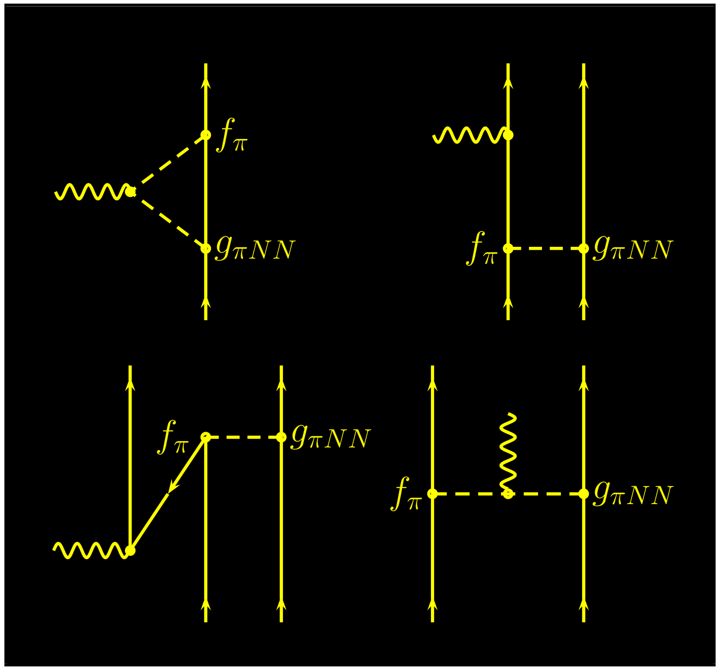

[11]B. Desplanques, J. F. Donoghue, and B. Holstein, Ann. Phys. (NY) **124** 449 (1980)

Constraints on Weak Coupling Constants

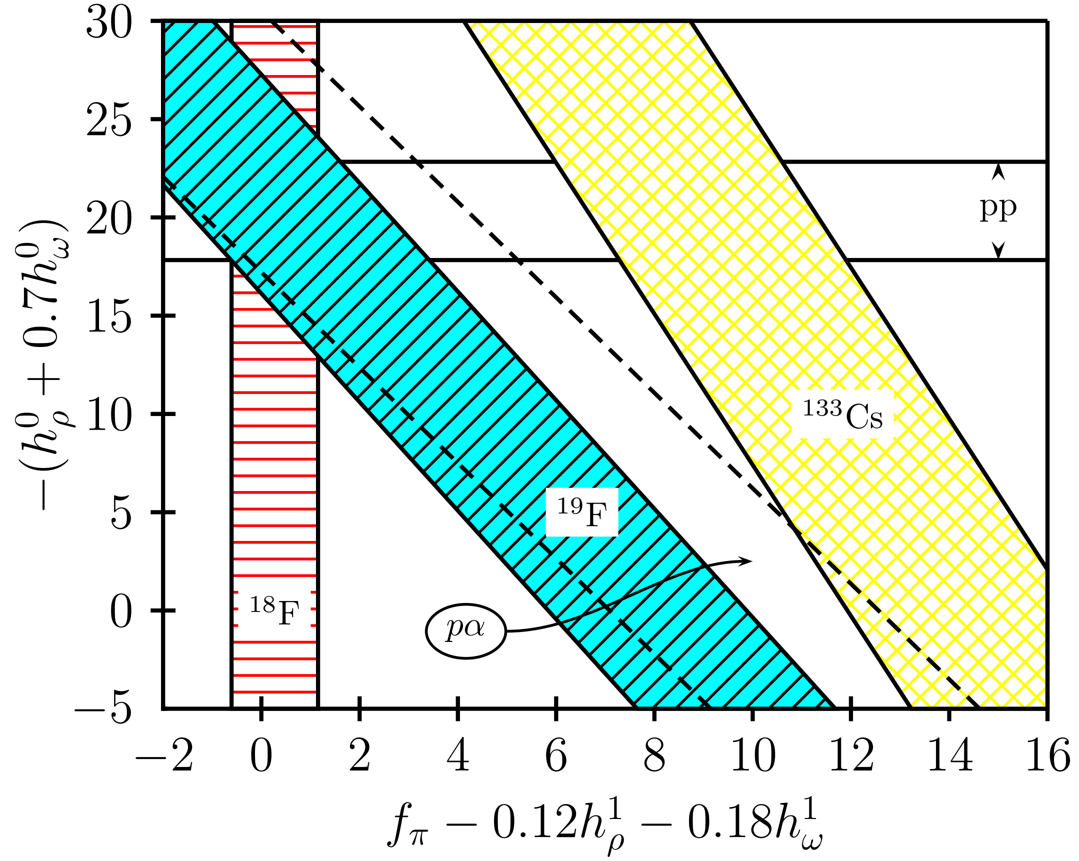

Microwave Experiments

The nucleon vector current does not contribute to transitions such as $|(6s\, I)F\rangle \rightarrow |(6s\, I)F'\rangle$ between different hyperfine components of an atomic level. Therefore, measurements of PNC between such levels directly measure the spin-dependent PNC amplitude.[12]

$$D = \langle (jI)F' \| ez \| (jI)F \rangle \ (i\kappa\ 10^{-12} ea_0)$$

Element	A	nl_j	I	D
K	39	$4s_{1/2}$	3/2	-0.222
Rb	87	$5s_{1/2}$	3/2	-1.363
Cs	133	$6s_{1/2}$	7/2	-17.24
Ba^+	135	$6s_{1/2}$	3/2	-6.169
Tl	205	$6p_{1/2}$	1/2	-30.00
Fr	211	$7s_{1/2}$	9/2	-237.9

[12] S. Aubin et al. 16th Int. Conf. on Laser Spect. (2001); S. G. Porsev and M. G. Kozlov, Phys. Rev. A **64**, 064101, (2001).

Conclusions

- Measurements of the weak charge in heavy atoms provide important tests of the validity of the electroweak standard model and provide limits on possible extensions.
- Measurements of the nuclear anapole moment provide constraints on nucleon-nucleon weak coupling constants.
- The measurements above must be combined with precise atomic many-body calculations to provide useful new information concerning weak interaction physics.